STM JOURNALS

Journal of
Materials & Metallurgical Engineering

ISSN: 2231-3818
Volume 16, Issue 1, 2026
January–Aprill
DOI (Journal): 10.37591/JoMME

https://journals.stmjournals.com/JoMME/

Research JoMME

Experimental and Simulation Study on Reduction Kinetics of Magnetite Ore by using Hydrogen

Vimal Sharma[1], Sanjeev Kumar Sarswat[2], Rakesh Prasad[3,*]

Abstract

In the present work, magnetite ore fines pellets were prepared for a study of reduction kinetics using hydrogen gas. In the present work, various parameters are investigated to assess their influence on reduction kinetics with respect to hydrogen utilisation. The different input variables influence the process, yielding the reduction fraction. The effect of temperature on reduction kinetics with hydrogen flow rate was explored for the optimum value of these parameters. The temperature is the key variable during the oxygen removal from the iron oxide compound. The breakdown of bonds from ferrous to solid iron molecules is dependent on the temperature of the reacting environment, which decides the rate of reduction. The reduction of magnetite ore occurs in two different segments. In the first phase of reaction, an intermediate phase, Wustite is formed, and then a stable compound is formed. For this study, Indian magnetite ore was chosen as the primary investigation for its chemistry through XRF, EDS and XRD. Ore fines were crushed to prepare four levels of fineness, such as 100, 200, 300, and 400 mesh, to make pellets for different categories. The study is focused on an alternative solution to conventional coke/coal reduction with pollution-free hydrogen gas as a reductant. A numerical simulation is used to validate the experimental data set, which supports the progressive development with less energy consumption. The reduction temperature range was 700-1000°C, and hydrogen flow rates were also investigated to assess their impact on reduction kinetics. To investigate the diffusion impact, non-linear curves were also examined for the pore diffusion influence on the reduction mechanism.

Keywords: Numerical simulation; Green steel Production; Hydrogen Reduction agent; Reduction Kinetics etc.

INTRODUCTION

***Author for Correspondence**
Rakesh Prasad
E-mail: sshaikh_gca@rediffmail.com

[1]M. Tech Student, Department of Mechanical Engineering, Vivekananda College of Technology and Management, Aligarh, Uttar Pradesh, India
[2]Assistant Professor, Department of Mechanical Engineering, Vivekananda College of Technology and Management, Aligarh, Uttar Pradesh, India
[3]Associate Professor, Department of Mechanical Engineering, Hindustan College of Science & Technology, Mathura, Uttar Pradesh, India

Received Date: April 14, 2026
Accepted Date: April 17, 2026
Published Date: May 04, 2026

Citation: Vimal Sharma, Sanjeev Kumar Sarswat, Rakesh Prasad. Experimental and Simulation Study on Reduction Kinetics of Magnetite Ore by using Hydrogen. Journal of Materials & Metallurgical Engineering. 2026; 16(1): 71–81p.

The carbon emission across the globe is a major issue; out of the total CO_2 emission, approximately 7% has been contributed by traditional carbothermic reduction. That impact is over the mounting pressure due to climate change activities in different ways. Paradoxically, to improve carbon efficiency, whatever activities have been employed, such as reducing the rate of coke, influence the content of CO_2/CO ratio in the environment. Hence, the carbon footprint per ton of production of iron increases yearly [1].

Due to this inherent limitation, the research possibilities into hydrogen as a safe and sustainable fuel and reductant were extended. That may be utilised independently or in the proper composition with CO, in order to make nearly zero emissions in

steel making [2]. However, hydrogen production via the root of steam methane reforming (SMR) is itself a carbon-based technique. It's a cost-effective carbon capture technique, where carbon storage and utilisation offer a more trusted decarbonization road map than the diffuse CO_2 emissions in the amount of thousands of tons from blast furnace operation [3]. The objective of the study is to mitigate the cost of hydrogen by diluting it with inert gases such as nitrogen and argon. Through the critical study, it is being explored how the partial pressure of hydrogen in the reduction of iron oxides will have an impact on the rates and efficiency of reduction kinetics [4].

India's gross iron ore reserves are estimated as 28.5 billion tons, consisting of approximately 10.6 billion tons of magnetite. So far, a major part of ore remains untapped; over hematite (Fe_2O_3) has been the key primary blast furnace feedstock globally, and the second part of ore, magnetite (Fe_3O_4), is underutilized. The avoidance of magnetite utility in the blast furnace due to its high density and low permeability creates a problem in the diffusion of the reducing gases [5].

Amid the reduction of hematite in the blast furnace, in the different steps ($Fe_2O_3 \rightarrow Fe_3O_4 \rightarrow FeO \rightarrow Fe$) more imperative compared to magnetite reduction. Due to porous structural stress developed through the transition of the hexagonal crystal lattice to the cubic crystal lattice, various cracks are generated and promote gas-solid interaction for reduction kinetics [6]. This intrinsic advantage of in situ-formed magnetite over natural magnetite has spurred recent interest in developing dedicated processes for its direct utilisation. In recent work on the kinetics of hydrogen reduction of magnetite ore in the blast furnace started. Wang and Sohn investigated high temperature reduction of magnetite concentrate with the temperature range 1150^0C – 1400^0C [7].

METHODOLOGY

The Indian iron ore was collected from Bhilwara, Rajasthan, which is magnetite ore. The chemistry of ore is shown in Table 1. A variable range of fineness of ore fines was prepared by grinding and crushing the ore in the ball mill.

Table 1. Iron Ore Chemistry

Bhilwara Iron Ore					
Ingredients	Fe_3O_4	Fe_{total}	SiO_2	Al_2O_3	LOI
Wt %	82.11	61.42	4.98	0.63	0.97

For the iron ore characterisation, EDS was conducted to ensure the oxygen amount carried by the iron ore at the initial phases of the study. For this, Rigaku, Bruker D8-Advance/D2-Phaser (2023) for powder samples, and Bruker Kappa APEX II (2005) were employed. The microstructural and elemental analysis obtained from EDS–SEM is shown in **Fig. 1**.

Initially, iron ore was ground to the above-mentioned particle size fraction to prepare iron ore pellets with a diameter of 8-10 mm. Since pellets may be larger than this, but to accommodate them in the reduction testing apparatus, a narrow size range was selected. The prepared pellets / experimental setup is shown in **Fig. 2**.

The purpose of the study is to study the reduction of iron oxide inside the blast furnace, conventionally, which happens in the presence of coke, and CO_2, CO gases are responsible for this phenomenon. Now, the oxygen content present in the iron oxide phases within the sample ore was measured by the technique of energy dispersive X-ray spectroscopy (EDS) as shown in Table 2.

Nova Nano FE-SEM 450 (FEI) provides ultra-high resolution characterisation & analysis, giving precise, true nanometer-scale information.

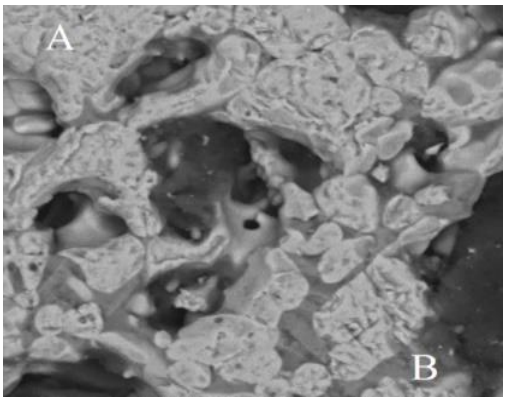

Figure 1. EDS -SEM

Table 2. Elemental composition (wt.%) of different phases (A and B) identified in pellets reduced at various temperatures (100°C, 200°C, 300°C, and 400°C).

PHASE	Wt.%	Pellet (a)	Pellet (b)	Pellet (c)	Pellet (d)
		100	200	300	400
A	Fe	65.51	67.91	62.26	61.15
	O	27.44	31.07	28.88	31.02
	Al	2.14	1.07	1.17	0.94
	Si	1.19	0	0.26	0.81
B	O	28.84	37.41	42.04	42.57
	Si	0.59	5.35	18.35	14.79
	Ca	0.6	4.38	17.14	12.29
	Fe	6.82	16.17	15.17	6.23
	Al	0	23.8	5.01	16.42
	Mg	0	3.23	4.66	1.09

Advanced optics & detection, including beam deceleration, in lens ETD (SE), TLD (custom), lens-mounted DBS & LVD, offer the best selection of information & image optimisation. It gives a resolution of 1.6 nm at 1 KV (TLD-SE) & <1 nm at 15 KV (TLD-SE). In this system, the EDS facility is also available.

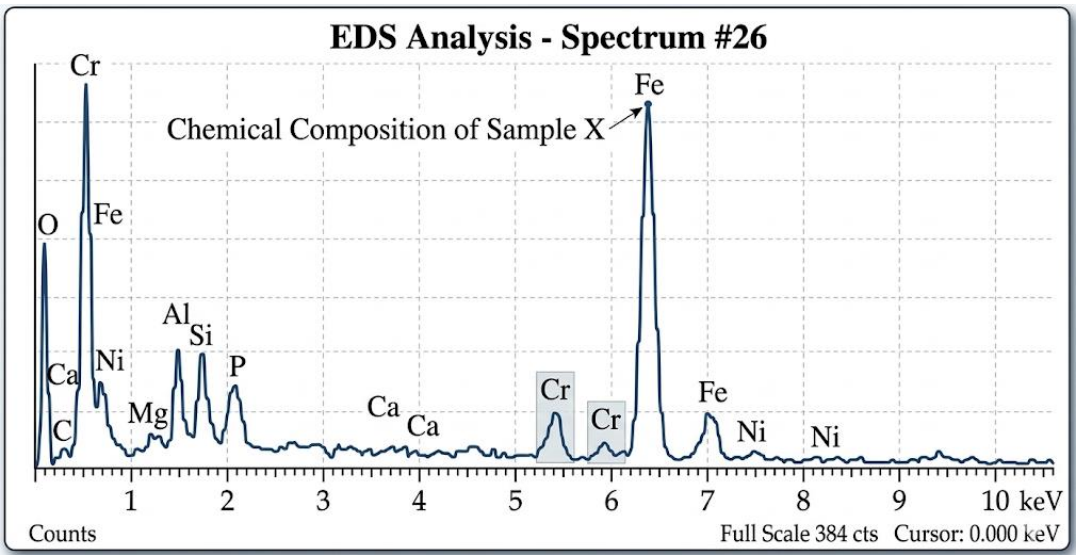

Figure 2. shows the different elements present in the ore sample

A Kinetic Model of Iron Ore Reduction

Thermodynamics of hydrogen reduction of magnetite (Fe_3O_4): a basic thermodynamic approach is mentioned here. According to thermodynamic principles, the Gibbs free energies of formation of compounds such as H2O, Fe3O4, and FeO are listed in data books based on their reaction equations [8].

$$\mathrm{Fe(s)} + \frac{1}{2\mathrm{O_2(g)}} = \mathrm{FeO(s)};\ \Delta G^{o} = -263720 + 64.35\mathrm{TJmol^{-1}} \quad \text{(a1)}$$

$$3\mathrm{Fe(s)} + 2\mathrm{O_2(g)} = \mathrm{Fe_3O_4(s)};\ \Delta G^{o} = -1108800 + 341.2\ \mathrm{T\ J\ mol^{-1}} \quad \text{(a2)}$$

$$\mathrm{H_2(g)} + \frac{1}{2\mathrm{O_2(g)}} = \mathrm{H_2O(g)};\ \Delta G^{o} = -247480 + 55.9\ \mathrm{T\ J\ mol^{-1}} \quad \text{(a3)}$$

The above three equations provide the free energy for the hydrogen reduction of Fe_3O_4 to FeO and FeO to Fe.

$$\mathrm{Fe_3O_4(s)} + \mathrm{H_2(g)} = 3\mathrm{FeO(s)} + \mathrm{H_2O(g)}\ ;\Delta G^{o} = 70160 - 92.25\ \mathrm{T\ J\ mol^{-1}} \quad \text{(a4)}$$

$$\mathrm{FeO(s)} + \mathrm{H_2(g)} = \mathrm{Fe(s)} + \mathrm{H_2O(g)};\Delta G^{o} = 16240 - 8.45\ \mathrm{T\ J\ mol^{-1}} \quad \text{(a5)}$$

The coexistence of all the solid phases at a common temperature for magnetite, wustite and iron that can be obtained by combining equation (a4) and equation (a5)

$$\mathrm{Fe_3O_4(s)} + \mathrm{Fe(s)} = 4\mathrm{FeO(s)};\Delta G^{o} = 54920 - 84.8\mathrm{TJmol^{-1}} \quad \text{(a6)}$$

The common temperature for all three phases at the same time in equilibrium 54920/84.8= 647 K. This indicates that in a Fe-saturated system, Fe_3O_4 can be stabilized at below 420°C while FeO is stable above 420°C. Therefore, below 420°C, Fe_3O_4 converts directly into FeO as per the transformation sequences as $\mathrm{Fe_3O_4} \rightarrow \mathrm{FeO} \rightarrow \mathrm{Fe}$ without intermediate FeO formation [9].

In the present study, the temperature range was kept at 700°C, 800°C, 900°C, and 1000°C during the reduction of iron ore at temperatures above 500°C. Therefore, Fe_3O_4 reduction is predictable and proceeds according to two-step equations.

The amount of hydrogen required to reduce the magnetite at a certain temperature can be computed as the thermodynamic efficiency of hydrogen utility. The number of moles of hydrogen is needed to remove the oxygen molecule from one mole of FeO. It is noticeable that in the ultimate thermodynamic step of reduction of manganite, the wustite transformation into iron (as shown in equation a5) [10].

For the consideration of reducing the number of moles of hydrogen is n, the equilibrium constant in equation (a5) at 1000°C, on the calculation of equation K can be obtained as 0.6, by using $\Delta G^{o} = -RT\ln K$. As per the equation, one mole of hydrogen with one atom of oxygen makes one mole of water, the remaining hydrogen molecule in terms of equilibrium constant $0.6 = \left(n_{\mathrm{H_2O}}/n_{\mathrm{H_2}}\right)_{\mathrm{eqbm}} = 1/(n-1)$. Finally, hydrogen moles of n = 2.67 are needed for one mole of effective hydrogen utilisation. This shows the thermodynamic efficiency of hydrogen $100(1/2.67) = 37.4\%$. Thus, one mole of Fe_3O_4 requires a total amount of hydrogen for complete reduction = 4 (oxygen atoms per mole of magnetite) × 2.67 (moles of hydrogen) = 10.68 moles of total hydrogen should be supplied [11].

As per the utilisation efficiency of reducing agent for iron oxides, CO require 12 moles to reduce one mole of Fe_3O_4, while hydrogen requires 10.68 moles less than CO. Secondly, hydrogen is environmentally friendly and an effective reducing agent to get iron from oxides. However, on the admitable table fact that hydrogen is costlier than CO gas for an economical process execution [12].

As per the above discussion, the reduction of magnetite (Fe_3O_4) by hydrogen occurred in two successive steps between the range of 700°C – 1000°C as per the equations below.

$$Fe_3O_4(s) + H_2(g) = 3FeO(s) + H_2O(g) \quad (A)$$

$$FeO(s) + H_2(g) = Fe(s) + H_2O(g) \quad (B)$$

The overall reaction from the equations is mentioned above.

$$Fe_3O_4(s) + 4H_2(g) = 3Fe(s) + 4H_2O(g) \quad (C)$$

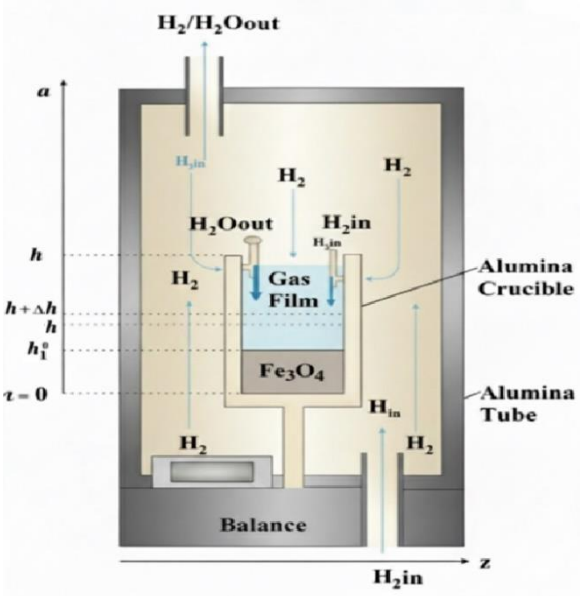

Figure 3. Reduction Apparatus

In this type of three kinetic steps gas-solid reduction analogy, as shown in the diagram of the reaction set-up in Fig. 3, in this apparatus, hydrogen enters at the inlet (mainly a mixture of H_2-H_2O) passing over the rectangular crucible containing the sample of iron ore oxide, leaving a gas film over the solid particle within the crucible. The gradient of concentration due to chemical reaction, developed across the gas film and gas diffusion of hydrogen and water vapour through the gas film will constitute the first step of the kinetic.

This is a form of gas film diffusion, in other words, a mass transfer step, governed by equation (a4). The rate of gas film diffusion kinetics is controlled by this equation [13].

$$X = \frac{C \cdot D_{H_2-H_2O}\left(x_{H_{2in}} - x_{H_{2eq}}\right)}{\left(h_2 - h_1^0\right)h_1^0 \cdot \rho_m} \cdot t = \frac{D_{H_2-H_2O}\left(C_{H_{2in}} - C_{H_{2eq}}\right)}{\left(h_2 - h_1^0\right)h_1^0 \cdot \rho_m} \cdot t \quad (1)$$

Where

X – fractional reduction of magnetite at the time of t instant;

$D_{H_2-H_2O}$ – diffusivity for binary gas H_2-H_2O;

C – molar concentration of the gaseous species

$C_{H_{2in}}$ – Hydrogen concentration at inlet

$C_{H_{2eq}}$ – Hydrogen concentration at equilibrium

$X_{H_{2in}}$ – Hydrogen mole fraction at inlet

$X_{H_{2eq}}$ – Hydrogen mole fraction at equilibrium

h_2 – crucible height

h_1^0 – initial bed height

ρ_m – molar density of magnetite ore

A significant fact is that $C_{H_{2eq}}$ is a non-zero quantity, due to the equilibrium constant of the second step (reaction (a2)). For the calculation of X, the following expression is used.

$$X = \frac{W(0)-W(t)}{W(0)\times 0.18842}$$

Where
$W(0)$ – initial mass of magnetite ore fines
$W(t)$ – mass at any given time t

Table 3. Pore Diffusivity

Temperature (°C)	Dpore (First Stage) (m^2/s)	Dpore (Last Stage) (m^2/s)
700	0.000022	0.0000282
800	0.0000401	0.0000534
900	0.0000572	0.0000931
1000	0.0000721	0.000142

The concept of pore diffusivity has been implemented in the present analysis, which directly influences the reduction kinetics. The value of D_{pore} for both stages is shown in Table 3.

XRF results indicate that 100 g of the iron ore sample contains 0.8832 moles of iron. According to the XRD data, 100 g of the ore sample contains 0.8832 moles of iron; the only iron-containing phase present is magnetite. Magnetite of 100 g sample contain the oxygen amount in mole 1.176 and 18.842 g, which can be count as a factor 0.18842 in the above expression of X. Apart from magnetite the other oxide such as SiO_2 has 6.15 % and Al_2O_3 has 4.7%, MgO has 0.39%, since during reduction, oxygen removal is the phenomenon, however they all are stable oxide including Cr_2O_3 contain 1.68% oxygen, due to their high negative, free energy formation. For simplicity, ideally, it is presumed that all the removal of oxygen is occurring only from magnetite iron ore; on that basis, X can be calculated accordingly [14].

In the first phase of reduction, a reduced iron layer or considerable thickness, this porous cover shell decides the unreacted oxide reduction. Diffusion through this layer will lead to the second kinetic step, which is termed the diffusion step. The diffusion governed kinetics rate equation is followed by equation (5a).

$$X^2 = \frac{2C\cdot D_{\text{pore}}\left(x_{H_{2\text{ in}}} - x_{H_{2\text{ eq}}}\right)}{h_1^{0^2}\rho_m}\cdot t = \frac{2D_{\text{pore}}\left(C_{H_{2\text{ in}}} - C_{H_{2\text{ eq}}}\right)}{h_1^{0^2}\rho_m}\cdot t \tag{2}$$

Where - D_{pore} is pore diffusivity factor

After this step, the third kinetics of the chemical interfacial reaction step will proceed. At the interface of unreacted ore and produce iron, a chemical reaction takes place [15]. The reaction-controlled kinetics of a chemical reaction are governed by equation (6a).

$$X = \frac{k_f'\left[C_{H_{2\text{ in}}} - \frac{C_{H_2O_{\text{in}}}}{K}\right]t}{\rho_m\cdot h_1^0} = \frac{C\cdot k_f'\left[X_{H_{2\text{ in}}} - \frac{x_{H_2O_{\text{in}}}}{K}\right]t}{\rho_m\cdot h_1^0} \tag{3}$$

Where

K_f' –first-order rate constant for forward reaction

$C_{H_2O_{in}}$ – H_2O Concentration at inlet

$X_{H_2O_{in}}$ – H_2O mole fraction at inlet

K – equilibrium constant

Governing equations eq. (a4) & (a5) depend on the reduction stages. These equations were constructed by mass balance of a small shell of thickness Δh along the vertical direction in the relevant diffusion zone, in the crucible. The detailed mathematical expression of the three rate equations (4a)–(6a) can be found in the respective paper [15].

NUMERICAL SIMULATION

In order to investigate the reduction of magnetite ore pellets, with different kinds of operating parameters, the process variables' influence on the reduction percentage with respect to time. Simultaneously, the other parameters are also investigated, like temperature and hydrogen flow rate, on the reduction fraction of magnetic ores. As per the governing equations of (4a)–(6a), the procedure follows the reduction kinetics as per the subjected conditions. Before experimental validation of reeducation kinetics, a numerical simulation is conducted to analyse the influence of process variables on the reduction fraction, under various circumstantial environments of reduction [16]. For this, the Python code was run in Google Colab. At the initial level, the effect of temperature was studied with respect to the time taken to perform the complete reduction of standard mesh 300 fines pellets with basic sample thickness (bed height) at 1 atmospheric pressure of hydrogen supply with the flow rate of 1 L/min for temperature variation. For the impact of the variation in the hydrogen flow rate on reduction percentage, the temperature of reduction was kept at 1000°C, and the pressure of hydrogen was kept at 1 atmosphere [17].

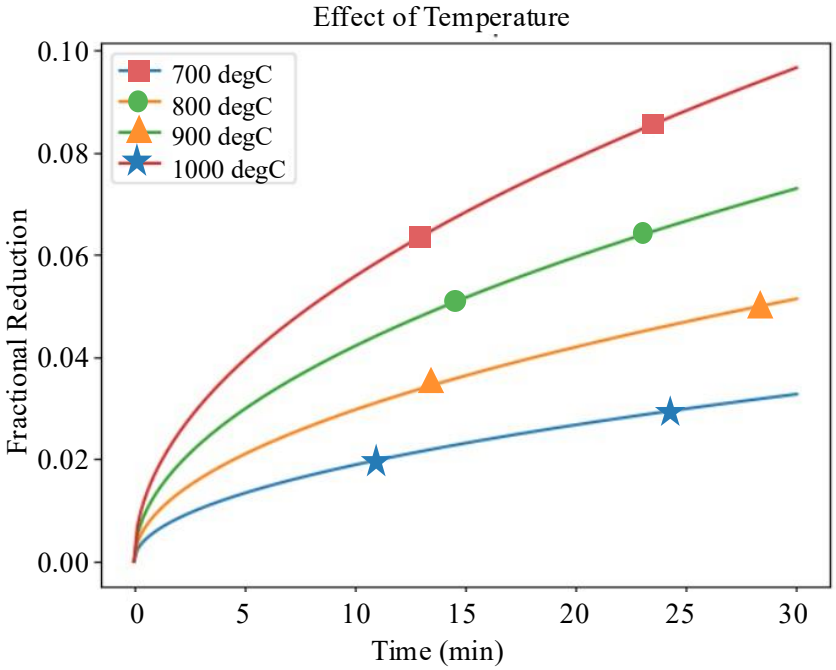

Figure 4. Numerical simulation curve- reduction fraction at different temperatures

As per Fig. 4, reduction fraction is completed at 1000°C, while for the other temperature range, 900 °C, reduction takes place partially. Observation states that at a lower reduction temperature, 600°C, the least fraction of reduction occurs.

As per Fig. 5, the reduction fraction variation at 1000°C, at 1 atmosphere, with a hydrogen flow rate was observed. The complete reduction took place at 1 L/min, and almost complete reduction takes place 0.8 L/min. while at the volume flow rates of 0.4 and 0.2 L/min, partial reduction takes place.

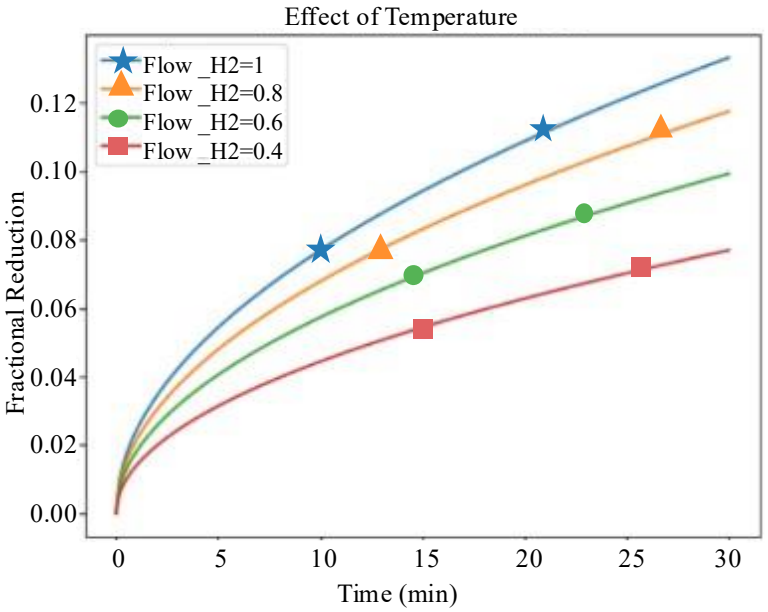

Figure 5. Numerical simulation curve- reduction fraction at different Hydrogen flow rates

RESULT AND DISCUSSION

Analysis of the micro compound with EDS spectra, magnetite ore reduction was done. As shown in Fig. 1, the XRF analysis is tabulated in Table 1. In the compound of magnetite, 33% oxygen and 61% iron ore content were recorded. Loss on ignition at 800-900 °C, 0.98 % in Table 1. The results obtained from various analyses have very minimal variability, such as oxygen content was 31.28% and iron content was 65.42%. Notably, magnetite reduction of iron ore pellets was considered on the basis of XRF results.

During reduction, bulk density plays an important role; in this study, four types of fines pellets have different bulk densities, as 2523 Kg/m^3, 2721 Kg/m^3, 3113 Kg/m^3, 3423 Kg/m^3 corresponding to 100, 200, 300, 400 mesh size. Apparent porosity 38%, 35%, 31%, 28% corresponding to 100, 200, 300, 400 mesh size as in Table 4.

Table 4. Effect of mesh size on bulk density and apparent porosity of pellets at different conditions (100, 200, 300, and 400).

Mesh size	**100**	**200**	**300**	**400**
Bulk density	2523 Kg/m^3	2721 Kg/m^3	3113 Kg/m^3	3423 Kg/m^3
Apparent porosity	38%	35%	31%	28%

Hydrogen Flow Rate Influence on Reduction

During the experiment of the reduction of magnetite ore pellets, the hydrogen flow rates are important parameters. Gas flow rates 0.4 L/min, 0.6 L/min, 0.8 L/min, 1 L/min were observed at 1000 °C at 1 atmospheric pressure, as shown in Fig 6.

With reference to Fig. 6, it was observed that a flow rate of 0.4 L/min of hydrogen offers slow reduction, and the final conversion of iron from ore is only 0.78, which is poor in indication. Flow rate 0.6 L/min shows a moderate fractional reduction, which is up to 0.83, the conversion of reduction with moderate efficiency. Hydrogen flow rate at 0.8 L/min, a fast speed of reduction occurred with

conversion of iron ore to iron up to 1, with good efficacy. Hydrogen flow rate at 1 L/min, reduction takes place at a very high speed, and conversion is reached up to 1, with the best efficiency [18]. Numerical simulation reveals the pattern of reduction of ore with respect to the hydrogen flow rate. In Fig. 5, the reduction variation is similar to the experimental observations. Thus, the numerical study supports the experimental study in saving time and cost of experimental execution for some conclusive facts.

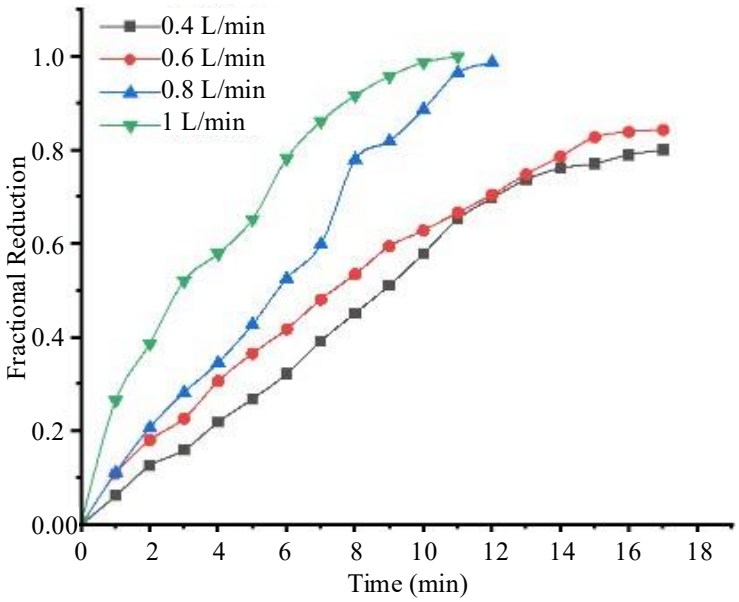

Figure 6. Reduction fraction over time for different hydrogen flow rates

Effect of Temperature

By fixing the other experimental parameters, such as pellet material, bed height (0.2 cm), particle size range (−125 + 106 μm), and hydrogen flow rate (0.4 L/min). At the constant parameters effect of temperature over the reduction rate (X) with respect to time (T) as shown in Fig. 7. It has been seen that in the first 24 minutes, reduction fractions 0.91, 0.96, 0.98, 1.0 were obtained with their respective reduction temperature 700°C, 800°C, 900°C, 1000°C respectively.

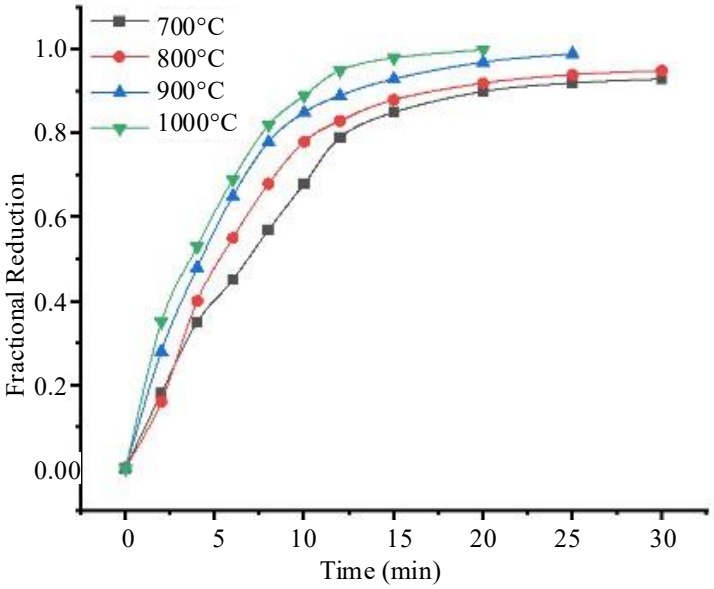

Figure 7. X versus T curves

In the X-T curves, the rate of reduction increased toward the higher-temperature end. This means a wider temperature range supports the reduction kinetics, resulting in a faster conversion rate as shown in Fig. 7.

With a very short duration of time, the reduction completion attained at the temperature 900°C and 1000°C, and their curve are closely spaced. This indicates that after the 900°C temperature, a less significant reduction rate was observed. Therefore, for further parameter study, 900°C was taken as the standard temperature for the present study, showing the almost complete reduction [19].

As per the numerical simulation technique, Fig. 4 shows the temperature effect on reduction fraction, with the highest reduction attained at a temperature of 1000°C. Reduction fraction almost at completion occurred for the temperature at 900°C, while at temperature 700°C, 800°C reduction was not properly efficient, same analogy was seen in the experimental study in Fig. 7.

As per the equation of the system eq. (4a) – (6a), it was expected that the relation between X and T should be linear. This is assumed for both gas film diffusion kinetics as per eq.(4a) or interface reaction kinetics as per eq. (6a). However, from the experimental data set, the X versus T plot is not linear, which indicates neither mechanism alone holds good for the overall reduction phenomenon [20].

CONCLUSION

This study demonstrated an environmentally friendly and sustainable alternative to replace coke and coal as a solid reducing agent in iron and steel making. Hydrogen provides the low molar requirement to reduce the same molar of iron oxide as compared to CO-based reduction. The reduction kinetics of iron ore has been investigated by a numerical simulation. The experimental analysis finds that the temperature and hydrogen flow rate directly affect the reduction kinetics. The theoretical aspect of numerical simulation was found very proper with the results of experimental study. Where higher values of temperature promote a fast rate of reduction, complete oxygen removal. The pore diffusion is the key controller of the reduction rate, as verified by X vs t and X^2 vs t plots analysis. The reduction occurs in two phases: Fe_3O_4 to FeO in the first phase and FeO to Fe in the second phase, with a transitional delay. At high hydrogen flow, reduction efficiency is improved by increasing mass transfer and maintaining an appropriate concentration gradient. The findings of the investigation state that around 900°C, at which complete reduction happened efficiently. Overall, this study contributes to optimising the hydrogen-based ironmaking technologies to promote carbon-free iron and steel making.

REFERENCES

1. Mallett A, Pal P. Green transformation in the iron and steel industry in India: Rethinking patterns of innovation. Energy Strategy Reviews. 2022 Nov 1;44:100968.
2. Zhang J, Shen J, Xu L, Zhang Q. The CO2 emission reduction path towards carbon neutrality in the Chinese steel industry: a review. Environmental Impact Assessment Review. 2023 Mar 1;99:107017.
3. Moulijn JA, Makkee M, Van Diepen AE. Chemical process technology. John Wiley & Sons; 2013 Mar 21.
4. Salucci E. Kinetic modeling of pure iron oxide powder reduction with hydrogen [doctoral thesis]. Åbo (FI): Åbo Akademi University; 2026. Available from: https://urn.fi/URN:ISBN:978-952-12-4675-3
5. Lee HG. Materials Thermodynamics: With Emphasis on Chemical Approach (With CD-ROM). World Scientific Publishing Company; 2012 Feb 28.
6. Wang H, Sohn HY. Hydrogen reduction kinetics of magnetite concentrate particles relevant to a novel flash ironmaking process. Metallurgical and Materials Transactions B. 2013 Feb;44(1):133-45.
7. Li P, Li Y, Yu J, Gao P, Han Y. Kinetics and microstructural changes during fluidized reduction of magnetite with hydrogen at low temperatures. International Journal of Hydrogen Energy. 2022 Aug 26;47(73):31140-51.

8. Miškovičová Z, Legemza J, Demeter P, Buľko B, Hubatka S, Hrubovčáková M, Futáš P, Findorák R. An overview analysis of current research status in iron oxides reduction by hydrogen. Metals. 2024 May 17;14(5):589.
9. Chatterjee R, Ghosh D. Kinetics of hydrogen reduction of chalcopyrite concentrate. Metallurgical and Materials Transactions B. 2015 Dec;46(6):2692-705.
10. Abolpour B, Afsahi MM, Azizkarimi M. Hydrogen reduction of magnetite concentrate particles. Mineral Processing and Extractive Metallurgy. 2021 Mar;130(1):59-72.
11. Gamisch B, Huber L, Gaderer M, Dawoud B. On the kinetic mechanisms of the reduction and oxidation reactions of iron oxide/iron pellets for a hydrogen storage process. Energies. 2022 Nov 7;15(21):8322.
12. Metolina P, Ribeiro TR, Guardani R. Hydrogen-based direct reduction of industrial iron ore pellets: statistically designed experiments and computational simulation. International Journal of Minerals, Metallurgy and Materials. 2022 Oct;29(10):1908-21.
13. Ali ML, Fradet Q, Riedel U. Particle-resolved computational modeling of hydrogen-based direct reduction of iron ore pellets in a fixed bed. Part I: Methodology and validation. International Journal of Hydrogen Energy. 2024 Oct 18;87:332-43.
14. Salucci E, D'Angelo A, Russo V, Grenman H, Saxen H. Review on the reduction kinetics of iron oxides with hydrogen-rich gas: Experimental investigation and modeling approaches. Industrial & Engineering Chemistry Research. 2024 Dec 16;64(1):1-35.
15. He K, Zheng Z, Zhu M, Gao X. Mesoscale simulation study and experimental analysis of the fluidized iron oxide hydrogen reduction process. International Journal of Hydrogen Energy. 2025 Feb 3;101:875-86.
16. Zhang J, Li S, Wang L. Kinetics analysis of direct reduction of iron ore by hydrogen in fluidized bed based on response surface methodology. International Journal of Hydrogen Energy. 2024 Jan 2;49:1318-31.
17. Meshram A, Govro J, OMalley RJ, Sridhar S, Korobeinikov Y. Modeling isothermal reduction of iron ore pellet using finite element analysis method: experiments & validation. Metals. 2022 Nov 25;12(12):2026.
18. Korobeinikov Y, Meshram A, Harris C, Kovtun O, Govro J, O'Malley RJ, Volkova O, Sridhar S. Reduction of iron-ore pellets using different gas mixtures and temperatures. steel research international. 2023 Oct;94(10):2300066.
19. Hammam A, Nasr MI, Elsadek MH, Khan IU, Omran M, Wei H, Qiu D, Yu Y. Studies on the reduction behavior of iron oxide pellet fines with hydrogen gas: mechanism and kinetic analysis. Journal of Sustainable Metallurgy. 2023 Sep;9(3):1289-302.
20. Hidalgo T, McDonald R, Beinlich A, Kuhar L, Putnis A. Comparative analysis of copper dissolution and mineral transformations in coarse chalcopyrite for different oxidant/lixiviant systems at elevated temperature (110°C and 170°C). Hydrometallurgy. 2022 Feb 1;207:105700.

